DETECTION OF DISTURBANCES IN THE AQUATIC ENVIRONMENT VIA DEEP LEARNING AND ARTIFICIAL NEURAL NETWORK INTEGRATED WITH STATISTICAL METHODS

Monik S. Sousa[1], Alan de C. Araújo[1], Yan F. da Silva[1], Aristófanes C. Silva[1], Alcione M. dos Santos[2] and João V. da Fonseca Neto[1]

[1]Department of Electrical Engineering, Federal University of Maranhão, São Luís, Brazil

monik.silva@discente.ufma.br, alan.carvalho@discente.ufma.br, yan.ferreira@discente.ufma.br, ac.silva@ufma.br, joao.fonseca@ufma.br

[2]Department of Public Health, Federal University of Maranhão, São Luís, Brazil

alcione.miranda@ufma.br

ABSTRACT

This study, two methodologies for detecting of oil slicks on the ocean surface are presented, based on the classification of images captured by the synthetic aperture radar. Grounded on these approaches, two algorithms were presented for the critical decision-making module of the system. The first, called LDA-MLP, combines classic techniques such as the linear discriminant analysis algorithm, with a multilayer perceptron neural network. This model does not process the image to build the predictive model, reducing processing time and is different from other classification methods. The second, known as DL-U-net, utilizes a more current technique, a neural network based on deep learning, U-net. This model performs image processing, like a filter, to eliminate noise and instances irrelevant to this classification. Based on the analysis of the results obtained, it is concluded that the methods of detecting oil slicks have good precision, LDA-MLP is simpler and has a shorter processing time.

KEYWORDS: *Linear Discriminant Analysis, Deep Learning, Artificial Neural Network, Oil Slick, Aquatic Environment Monitoring.*

I. INTRODUCTION

Despite having been known since ancient times, petroleum exploitation and refining became significant only at the end of the 19th century with the production of kerosene. When kerosene was produced, the heavier fraction (residual until then) was discovered to be a fuel for use in boilers and heating (replacing coal); thus, fuel oil was generated. However, it was not until early 1912 that fuel distribution began in Brazil with the arrival of the Standard Oil Company [1].

Most reserves of oil and its derivatives are in offshore fields, which have led to drilling activities reaching greater depths. According to the Brazilian Statistical Yearbook of Petroleum, Natural Gas, and Biofuels for 2022, in 2021 the volume of oil produced worldwide increased by 1.6% compared to 2020, reaching 89.9 million barrels per day [2].

These production activities in the oil and natural gas sectors generate high economic growth in the country. However, these processes have major environmental impacts, such as oil spills, interference with water resources, and community insecurity.

Owing to the growth in the oil industry, several accidents have occurred worldwide, resulting in the release of toxic or flammable substances. These incidents have caused severe environmental damage to fauna and flora, as well as deaths and damage to the health of the population living near the accident sites. According to the 2022 Petrobras sustainability report, in Brazil, nine events involving oil and derivatives spills were recorded, totaling 218.03m3, a value 82% higher than the alert limit stipulated for the year [14].

Consequently, this has encouraged countries and companies to enhance their environmental regulations for maritime transportation, as well as the operation, monitoring, and conservation of pipelines for hydrocarbon transportation. These efforts involve adopting methods and techniques that are less aggressive to the environment. By seeking systems capable of detecting, tracking, and locating oil leaks, companies can act quickly and effectively to reduce environmental damage.

The detection of oil slicks in the ocean is a critical environmental issue. When carrying out the literature review, several methods, tools and techniques were identified that help in monitoring and detecting areas affected by this type of accident, using synthetic aperture radar images. (SAR), due to its advantages, which are the ability to penetrate clouds and provide high-resolution images. SAR, mounted on aircraft or satellites, is a microwave-based technology that emits pulses of radiation toward the ocean surface and receives its reflection to capture a representation of the scene. This is currently the most used method due to its precision, fast data acquisition and large simultaneous coverage area [3].

Another technique that has been highlighted in this area is the wireless sensor network (WSN), which is a network of autonomous sensor devices that communicate over wireless channels. These networks consist of multiple sensor nodes (static and dynamic) with multiple sensors per node that communicate with each other and the base station over wireless radio links [4].

Various methods are proposed to detect oil slicks using SAR images [5] [15] [16] [17] and convolutional neural networks (CNNs) have been widely adopted. They are deep neural networks, used to classify images, group them by similarity and perform object recognition within a scene. The effectiveness of CNN in image recognition is one of the main reasons why deep learning has gained prominence. Some architectures used to perform this detection ResNet-101, U-net, LinkNet and DeepLabv3+ [5].

Dongmei Song [7] proposed a methodology that uses ANN with statistical methods for the detection of oil spills, using PolSAR images (polarmetric synthetic aperture radar). This model consists of a CNN for extracting deep features from the original data, performing dimension reduction and reducing data redundancies. These features are then merged through Principal Component Analysis (PCA), and the Support Vector Machines (SVM) are used to perform the classification. The results obtained with this proposed method showed good classification accuracy, with a more accurate oil spill detection, that is, with a low rate of false alarms.

In reference [19] proposes a method based on linear discriminant analysis (LDA) to improve the performance of Global Navigation Satellite System-Reflectometry (GNSS-R) sea ice detection, in terms of accuracy and robustness to noise. This method showed an accuracy of 95.03% for data with low noise effect. However, it still proved to be more robust for data with medium and high noise effect than the CNN-based method.

In view of the above, the proposal presented in this study aims to develop two methods for the detection and classification of oil slicks on the ocean surface. These methods are based on the integration of statistical techniques and artificial neural networks (ANN), whereas the theoretical foundations of the other methods are based on deep learning. In terms of application, the proposed algorithms are customized for processing satellite images for the detection and classification of oil slicks on the ocean surface.

Consequently, this study seeks to contribute to the monitoring and mitigation of harmful effects caused to the environment by humans. Efficient monitoring and preventive alerts are necessary to combat these

risks and limit environmental damage. In addition, we propose a methodology for detecting exogenous disturbances in aquatic environments. The proposed methodology is oriented towards the development of methods, procedures, and algorithms for the detection/classification problem. Thus, this methodology can be applied to the WSN. For example, local and online port monitoring via WSNs can detect the presence of oil stains in a docking zone.

Two methods for oil slick detection in an aquatic environment the paper presents, one using statistical methods with a neural network and the other using a neural network with deep learning. Section II describes the oil-slick detection system. The analysis methods and algorithm construction for the critical detection system are presented in Section III. A performance evaluation of the detection results and a ranking of the proposed methodologies are presented in Section IV. Finally, Section V concludes the paper.

II. OIL STAIN DETECTION SYSTEM

This section presents the development of a signal-processing module for anomaly detection in aquatic environments. The problem was investigated, and the proposed solutions were contextualized using the block diagram shown in Figure 1, which is a diagram of the system for oil slick detection on the ocean surface. The system is made up of five functional blocks: a) process, which is the subject of monitoring; b) disturbances, which are the agents that cause changes in the process; c) measurements, which involve devices or equipment responsible for acquiring information (signals); d) critical, which is the device or sensor node that evaluates the impact of the disturbance on the process; e) decision making, which is the unit responsible for planning and executing tasks based on the critic's assessments.

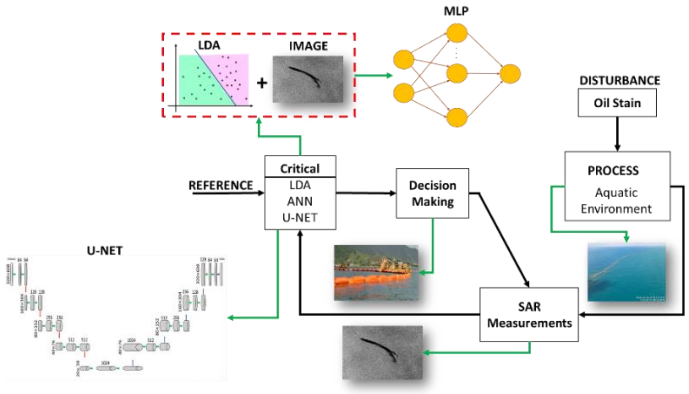

Figure 1. Block diagram of the oil slick detection system on the ocean surface

According to the block diagram in Figure 1, the oil detection system in a water environment incorporates a reference signal (a clean and spotless water environment) that provides a parametric representation of the value function based on the measurement data. Consequently, the proposed detection method is geared to be embedded into the critical detection algorithm, which is responsible for detecting anomalies during the process.

The process being monitored is an aquatic medium. Oil slicks are considered process disturbances, and the measurements of the aquatic medium are obtained from the monitoring. To monitor the aquatic environment, SAR images are used because they are minimally affected by the sun and cloud rays and possess the ability to capture images throughout the day and in any climate with a wide range and high resolution [18].

The information from the SAR is input into the detection algorithm. The measurement signals are processed using methods and techniques, such as multivariate data analysis, ANN, and deep learning. In addition, as shown in the block diagram in Figure 1, the information flow from the critic is sent to the decision-making module. If oil slicks are detected on the ocean surface, these measures are applied by an external individual. This involves implementing an appropriate control policy to contain the slicks and clean up the affected aquatic environment to minimize environmental impacts. This decision is not

part of the proposed detection system.

III. ALGORITHMS FOR A CRITICAL DETECTION SYSTEM

In this study, two methods for the detection and classification of oil slicks on the ocean surface are presented: LDA–MLP, which uses the integration of statistical methods, such as linear discriminant analysis (LDA), artificial neural networks, and multilayer perceptron (MLP). The second method is based on deep learning (DL-U-net) and uses the convolutional neural network in the U-net architecture.

3.1. CRITIC'S LDA-MLP MODEL

The LDA-MLP algorithm proposed for the detection of oil slicks on the surface of an aquatic environment consists of the following steps: capturing the images, estimating the class to which each image belongs, and classifying the input data using the estimate provided by LDA [21]. The proposed method does not process the image to build the predictive model. This approach helps to reduce the processing time. It differs from other classification methods, which first perform an entire image treatment, eliminate noise, and perform image segmentation. Figure 2 presents the functionality of each step-in block form and the trajectories of the information flow for detection using the proposed algorithm.

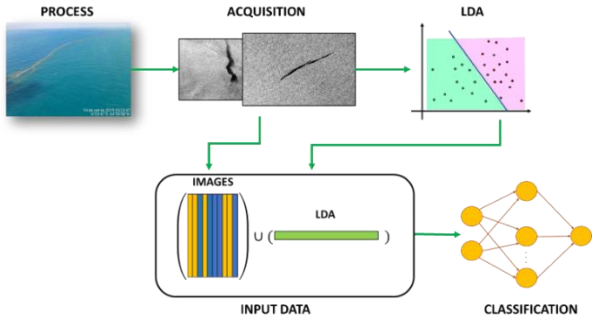

Figure 2. Scheme of the LDA-MLP oil slick detection algorithm

According to the scheme shown in Figure 2, we have the process that in this case study is the ocean surface, as previously mentioned in the block diagram of Figure 1, representing the aquatic environment. The oil slicks are considered disturbances. It is necessary to acquire images of the ocean surface, that is, the surface to be monitored, without first performing any processing on the image. Thus, the SAR images are used in their original form as received from the satellite.

The classes are then estimated using the LDA technique, in which the classes to which the image belongs are calculated from the response of the Fisher discriminant function, which is added to the concatenated vector of the image; each vector consists of the image data plus the estimate of which class the image belongs to.

The linear discriminant analysis aims to distinguish the groups (or classes) of the dependent variable through independent variables; that is, it intends to discover the characteristics (explanatory variables) that distinguish between members of different groups so that, when the characteristics of a new case (individual) are known, it is possible to classify which group of the dependent variable it belongs to [8].

The Fisher discriminant function for this two class problem is given by

$$D(x) = Lx, \tag{1}$$

where x is the vector of population characteristics and L is the estimated discriminant vector for the two classes, which is given by

$$L = (\mu_1 - \mu_2)'\sum^{-1}, \tag{2}$$

where μ_1 is the class average C_1, μ_2 is the class average C_2, and $\sum$ is the common covariance matrix for the two classes. Assuming that the covariance matrices of the classes are equal, then

$$\Sigma = \left[\frac{(n_1 - 1)}{(n_1 - 1) + (n_2 - 1)}\right] cov_1 + \left[\frac{(n_2 - 1)}{(n_1 - 1) + (n_2 - 1)}\right] cov_2, \quad (3)$$

where n_1 is the number examples from C_1, n_2 is the number examples from C_2, and cov is the covariance matrix of each class, which expresses the dispersion of the class data. It is desired that this dispersion be as small as possible, so that Fisher's discriminant function can minimize the probability of misclassification. To apply the classification rule and obtain the estimate of the classes, the midpoint between the means of the two populations is calculated as

$$m = \frac{1}{2}(\mu_1 - \mu_2)'\Sigma^{-1}(\mu_1 - \mu_2). \quad (4)$$

This classification rule states that if $D(x)$ is greater than m, image examples x belongs to class C_1; otherwise, examples image x belongs to class C_2. Then, classification is performed using the MLP neural network, which separates the images into two groups: surfaces with oil slicks and clean surfaces (without oil slicks).

The MLP consists of an input layer that receives the data to be processed by the network and hidden (or intermediate) layer(s). In this study, there is only one hidden layer. Finally, there is the output layer that returns the answer. The number of neurons in this layer is related to the task that the network is performing [9]. The algorithm used for training is backpropagation, which is based on error-correction learning heuristics, in which the error is backpropagated from the output layer to the intermediate layers of the network. This algorithm operates in two steps: the forward phase, which calculates the synaptic weights of the neurons based on the input layer data to produce the response in the output layer, and the backward phase, in which the output is compared with the desired output. If there is an error, it is propagated from the output layer to the input layer, and the weights of the intermediate layer neurons are modified as the error is backpropagated [9].

The training process of the MLP is the same as that of a single-layer perceptron, in which the output of layer one is input to layer two, and so on, until the output layer of the neural network is reached. The difference between the desired value and output of the network indicates the error made by the network for the input data, which is used in the backward phase to adjust the synaptic weights of the network. All these steps of class estimation with classification occur in the block of the critic, as illustrated in the block diagram of the detection system (Figure 1). Consequently, in the context of the decision-making system shown in Figure 1, the main features of the functional blocks of the critical algorithm for oil slick detection are presented in Figure 2.

3.2. CRITIC'S DP-U-NET MODEL

The second algorithm, proposed for the detection of oil slicks on the surface of an aquatic environment, consists of a set of steps: image capture, image processing, and classification of the input data. Therefore, in contrast to the classification by the proposed method using the LDA-MLP approach, this method performs processing on the image, such as a filter and some adjustments, to eliminate noise and instances that are not of interest for this classification before using it to build the model of the convolutional classifier. For the proposed algorithm, Figure 3 shows the processing steps for oil slick detection on the ocean surface in the form of a flowchart, which is based on the DL-U-net algorithm.

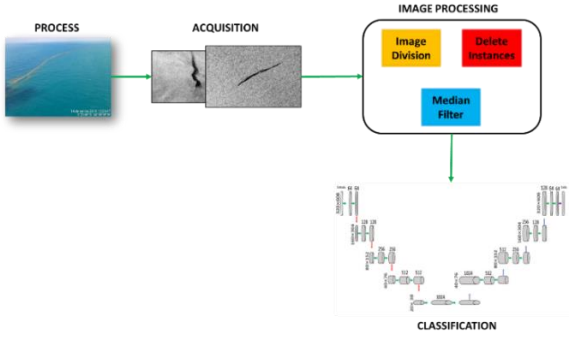

Figure 3. Scheme of the DL-U-net oil slick detection algorithm

According to the scheme in Figure 3, the process being monitored is the ocean surface, and the initial step involves acquiring images of the ocean surface. Because the SAR images obtained have a large dimension, the image is divided into four, and the other instances of the image are eliminated, leaving only what is desired to detect the oil slicks. In addition, the acquired images often contain noise, making it difficult to interpret them; therefore, they undergo processing to attempt to eliminate as much noise as possible.

After processing the database, the images are ready to train a deep neural network using the U-net architecture. After the training is performed, a test is conducted to analyze the efficiency of the trained classifier. These image processing and classification steps are represented in the block diagram of Figure 1 by the critic block.

With deep learning, it is simpler for an algorithm to perform tasks that were previously extremely difficult, such as recognizing objects in an image. Convolutional neural networks (CNN) are responsible for bringing deep learning to the forefront because they have proven to be efficient in accurately classifying pixels [10].

Other deep networks have been developed from CNN, such as U-net [11] and DeepLabv3+ [5], and have been applied to image classification and segmentation. The U-net network is a fully convolutional network, which has the characteristic of being faster because it avoids the use of denser layers and many parameters, allowing its use for any image size. In this network, there is an initial sampling reduction because a convolutional filter is applied that contracts the image at different resolutions and filters, and detects different structures and textures. In the second stage, a resolution increase is performed, making interconnections between images and equivalent scales, and generating better image quality [12].

IV. DETECTION AND CLASSIFICATION RESULTS

To evaluate the performance of the proposed detection methodology, images from the Oil Spill Detection Dataset (MKLab) were used. The database consisted of SAR images. A description of the experiments and analysis of the results of the two proposed methods for detecting oil slicks in the ocean are presented in this section. The first algorithm integrates statistical methods and an artificial neural network, namely the LDA-MLP classifier. The second method originates from deep learning (DL), which is the DL-U-net classifier. By implementing these algorithms, a software/code product was obtained to detect oil slicks on the ocean surface. Both classifiers are designed to compose the software core of the critic module, as shown in Figure 1.

4.1. DATABASE

The database used was the Oil Spill Detection Dataset (MKLab), which contains 1.112 images depicting instances of five classes, including oil spill, look-alike (which looks like an oil slick but is not), land, ships, and marine areas [5]. These images were acquired through the European SENTINEL-1 satellite mission, which is applied for land and ocean monitoring, equipped with the SAR radar sensor, which is an active system, can capture images all day long, and does not suffer from fog or dust. It operates in the c band, that is, it uses a frequency spectrum between 4 and 8 GHz to communicate, this communication band is preferred, as it allows information to continue to travel even under adverse weather conditions [20].

The ground range coverage of the SAR sensor used in the SENTINEL-1 mission was approximately 250km with a pixel spacing of 10×10m. This radar system covers large areas of interest and captures relatively small instances. The polarization of the employed system is dual, that is, transmitted vertical polarization - received vertical polarization (VV) and transmitted vertical polarization - received horizontal polarization (VH). Consequently, this radar can transmit in vertical polarization and receive in both vertical and horizontal polarization, which allows different types of targets to be obtained.

The SAR imagens of this database were captured in the period from September 28, 2015, to October 31, 2017. Information on the geographic coordinates, date, and time of the pollution events was provided by the European Maritime Safety Agency (EMSA) through the CleanSeaNet service. To build the database, only the raw VV band data were processed, following a series of preprocessing steps to

extract common visualizations, as it is a specialized database for oil spill detection [5]. The captured images were resized to 1250×650 pixels.

The database also contains image masks that depict the instances present in the image, such as oil slicks and ships, using different colors to represent each of the five classes. Figure 4 shows the SAR image and its corresponding mask.

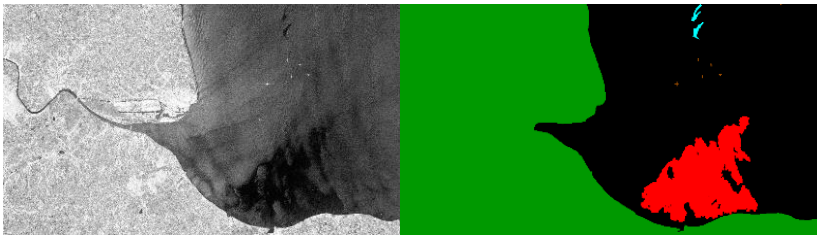

Figure 4. Database images: SAR image, mask

The black spots in the SAR image that cover large areas of the images are usually related to look-alikes (which resemble oil slicks) as opposed to the dark, elongated spots that are oil spills, as shown in Figure 4; however, this is not always the case. Consequently, the detection of an oil slick is a significant challenge because the shape of the oil slick is ambiguous.

In the mask shown in Figure 4, green represents land, black represents the ocean surface, brown represents ships, red represents sailfish, and cyan represents oil slick. These masks are important for the training and evaluation of nets used to detect oil slicks.

When building a classifier, and test set is used to validate the classifier, the training set is previously known and used to extract knowledge and build the classifier model [13]. In this study, the database was divided into 1002 images for training and 110 images for testing. In total, there were 879 images with oil slicks on the ocean surface, which amounted to 79.05% of all data, and 233 clean images without oil slicks, which amounted to 20.95% of the entire database.

These SAR images are significantly affected by speckle noise, which is a multiplicative noise proportional to the intensity of the received signal. Its visual effect is a grainy texture that can make it difficult to interpret the images. Therefore, many researchers perform image processing to improve the image quality before using them to obtain the predicted model. These processing techniques aim to eliminate noise, emphasize edges, and smooth the image. Another technique widely used by researchers is segmentation because it divides images into regions, which helps in classification. However, this study presents both scenarios: tests performed without any preprocessing of the images and tests performed with preprocessing of the database.

4.2. Statistical Analysis

Before applying any technique to process the information in the database, it is necessary to perform data analysis, because this analysis provides information about the behavior of the classes, indicating whether it is possible to separate the two classes. The data of the classes were analyzed in terms of their distribution and variance.

To analyze the distribution of images and determine whether there is a similarity in the distribution of the two groups, it is of utmost importance to predict whether the two groups are separable. For this analysis, one image from each group was randomly selected, and their histograms were plotted, as shown in Figure 5. The x-axis represents the pixel value, which ranges from 0 to 255, and the y-axis represents the frequency of the pixel value that appears in that image.

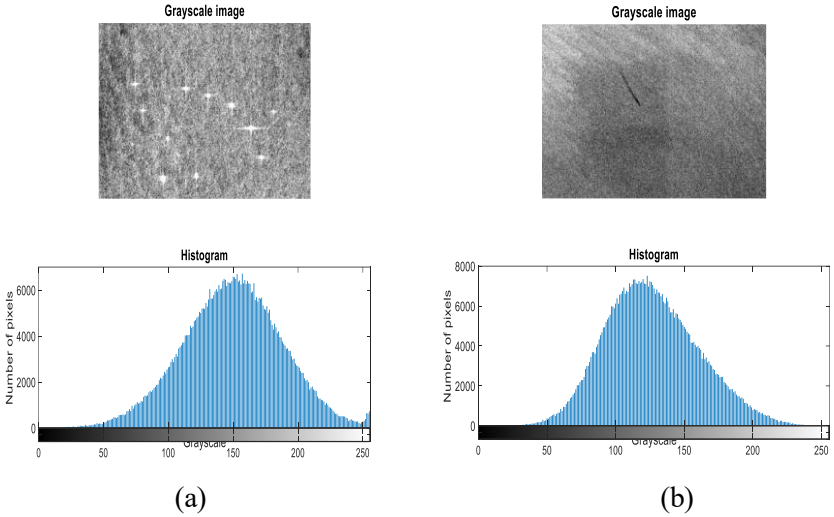

Figure 5. Histograms of the SAR images: (a) images without oil stains, (b) imagens with oil stains

According to Figure 5, the histogram of the image without oil slick on the ocean surface has its peak is closer to 150 and more pixels are closer to white. The histogram of the image with oil slick has its peak is close to 100, indicating that there are more pixels in the darker color closer to the black color. Consequently, there was a difference in the distributions of the two groups. In addition, the histograms show the characteristics of a normal distribution, which is the reference distribution for the statistical methods used in this study.

The second analysis performed on the data was the homoscedasticity analysis to check the variances. Similar to the normality analysis, a graphical analysis was performed using the box plot, which provided information about the location, dispersion, asymmetry, tail length, and outliers of the data set. Specifically, the average of each class was calculated, with the training database, then the box plot was then plotted for the two groups, to analyze the variance between groups, as shown in Figure 6.

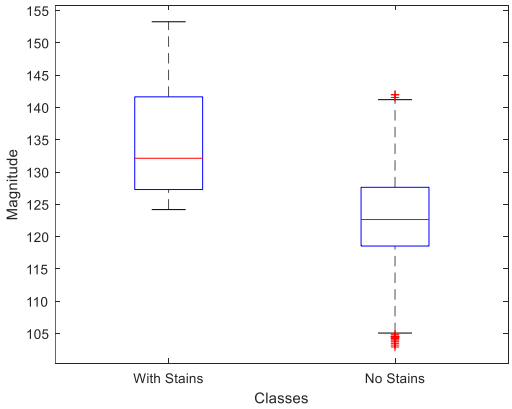

Figure 6. Boxplot of the two groups

In Figure 6, there is the x-axis representing the classes; the group with oil stain, and the group without oil stain. On the y-axis we have the magnitudes of the pixels of the images. When analyzing the graph, it is observed that the notches of the two boxes do not overlap, which indicates that the median pixels of the images with oil stain and without oil stain are significantly different. Additionally, the median (red line in the box) of the group of images with spots is not centered, it has a value of 132.13, which indicates that each sample is slightly skewed. The group without oil spill has its median centralized, assuming a value of 122.65, but it presents outliers, while the other group does not have any outliers. These outliers are due to the members who are also shown with dark spots in the SAR image, hence the difficulty in detecting oil stains correctly.

4.3. LDA-MLP Model Design

As mentioned above, the LDA–MLP model has three steps: the acquisition of the images, the estimation of the classes by the LDA technique, and the classification through the MLP network, which has the concatenated vector of the images plus the LDA estimate as input. The outputs of the classifier were 0 (clean ocean surface) and 1 (oil-slick ocean surface), and these values were compared with the desired output to verify the efficiency of the model.

The algorithm for image classification of a clean or oil slick ocean environment developed for this ocean surface oil slick detection system is divided into two: the LDA and MLP algorithms. The first algorithm reads images from the training database and uses the average of each class to calculate the covariance matrices of the classes and common covariance matrix. Using these matrices, a discriminant function is built to arrive at the classification step, and its code is exposed to Algorithm 1 - LDA.

ALGORITHM 1 - LDA

- **Startup**

Read the images;
Resise the images;

- **LDA**
  - **Average of each class**

$$\mu_j \leftarrow \frac{1}{n_j} * \sum_{j=1}^{n_j} x_{ij};$$

  - **Covariance matrix**

$$\phi_j \leftarrow I_j - \mu_j;$$

$$cov_j \leftarrow \frac{\phi_j * \phi_j'}{n_j - 1};$$

$$\Sigma \leftarrow \frac{1}{(n_1 - 1) + (n_2 - 1)} * \sum_{j=1}^{c} (n_j - 1) * cov_j;$$

  - **Midpoint between classes**

$$m \leftarrow \frac{1}{2} * [\mu_1 - \mu_2]' * \Sigma^{-1} * [\mu_1 - \mu_2];$$

  - **Discriminating vector**

$$L \leftarrow [\mu_1 - \mu_2]' * \Sigma^{-1};$$

  - **Discriminating function**

$$D(x) \leftarrow L * x;$$

  - **Classification**

$$\begin{cases} D(x) \geq m \rightarrow C_1 \\ D(x) < m \rightarrow C_2 \end{cases}.$$

- **End of algorithm**

According to the LDA algorithm, the images are resized to 63×33 to minimize the computational effort. μ_j is the mean of class j, x_{ij} are the samples of class j, n_j is the number of samples of class j, c is the number of classes, cov_j is the covariance matrix of class j, and Σ is the common covariance matrix between the classes. L is the discriminant vector consisting of the parameters of the function. These parameters generate a better separation between the classes. D denotes the Fisher discriminant function, x is the test data, which contains both oil slick and clean ocean surface images, and m is the midpoint used in Fisher classification.

After applying LDA, two data points are used to perform the analysis: the first analysis uses the class estimate, and the second analysis uses the response of the discriminant function. This information is added separately to the hues of the input images. Therefore, the new image vector becomes 2080×1 in dimensions as an additional piece of information is added, which is the image class estimate or discriminant function response.

The algorithm for oil slick detection using the multilayer perceptron neural network consists of three steps: the acquisition of the aquatic environment that is being monitored (SAR images), the training, which is the part of the algorithm in which the weights are adjusted so that the classifier is as close as

possible to the ideal, and the test to verify the efficiency of the classifier. These steps are presented in Algorithm 2 - MLP.

ALGORITHM 2 - MLP

- **Startup**

1 $Load\ data;$
2 $Read(data);$
3 $X_{Train_1}(i,:) \leftarrow data(training) \cup D(training);$
4 $X_{Train_2}(i,:) \leftarrow data(training) \cup C(training);$
5 $X_{Test_1}(i,:) \leftarrow data(test) \cup D(test);$
6 $X_{Test_2}(i,:) \leftarrow data(test) \cup C(test);$
7 $d_{Train} \leftarrow classes;$
8 $d_{Test} \leftarrow classes;$
9 $W \leftarrow \begin{bmatrix} 0 \\ \vdots \\ 0 \end{bmatrix}_{(l+1)\times 1};$
10 $epoch = int;$

- **Iterative Process**
  - **Weighted Sun**

11 $Y_t \leftarrow \sum_{i=1}^{K} W * X_{Train_t}(i,:);$

  - **Activation Function**

12 $R_t \leftarrow ReLU(Y_t);$

  - **Weight Update**

13 $IF\ d_{Train} \neq Y_t\ THEN$
14 $\Delta W_t \leftarrow \eta * \left(d_{Train}(i) - Y_t(i)\right) * X_{Train_t}(i,:);$
15 $W_t \leftarrow W_t + \Delta W_t;$

  - **End Loop**

- **Iterative Process - Test**
  - **Weighted Sun**

16 $u_t \leftarrow \sum_{i=1}^{K} W_t * X_{Test_t}(i,:);$

  - **Activation Function**

17 $IF\ u_t < 0\ THEN$
18 $RES \leftarrow 0;$
19 $IF\ u_t > 0\ THEN$
20 $RES \leftarrow 1;$

  - **End Loop**

- **End of Algorithm**

According to the MLP algorithm, the variable data is the database with the 1112 images. X_{Train_t} is the matrix with the training images that contains 1002 images plus the LDA information, which can be the estimate of the classes or the response of the discriminant function, in which each column corresponds to an image. d_{Train} is the vector of desired outputs, W_t is the vector of synaptic weights, $epoch$ is the number of iterations, u_t is the weighted sum response, Res is the perceptron output, η is the learning rate, ΔW_t is the difference calculated according to the classification error to update the synaptic weights, and X_{Test_t} is the matrix with the images and the LDA information for testing the classifier.

4.4. Result from the LDA-MLP Model

When receiving the database, the only operation performed on the images was a reduction of dimension from 1250×650×3 to 63×33 because the image dimension was too large, leading to higher memory consumption and processing time of the algorithms. In addition, as the images are in grayscale, it does not require a three-dimensional matrix. The linear discriminant function was then calculated, using this training database. The calculated discriminant function had a hit of 100%, that is, it had a true positive rate of 100% and a false positive rate also of 100%.

To verify the performance of the discriminant model, experiments were conducted using a test database containing 110 images. These analyzes were performed based on the evaluation metrics; as accuracy that indicates the percentage of correctness of the predicted model, the precision that indicates the percentage of correctness of the positive class in relation to all data classified as positive, recall that indicates the percentage of success of the positive class in relation to the data that really positive, and the F1 metric which is a balanced harmonic mean between precision and recall [6]. The values obtained for these metrics are listed in Table I. Another metric analyzed is the ROC curve that presents the true positive rate versus the false positive rate, a way to assess the quality of the predicted model to distinguish between the two classes.

According to Table I, the calculated discriminant function of the LDA shows a correct classification of 87.50% of the images with oil slicks and 100% of the images without slicks. The ROC curve is a graphical technique used to evaluate the ability of the predictive model and make the proper classification, and the ROC curve of this predictive model is shown in Figure 7.

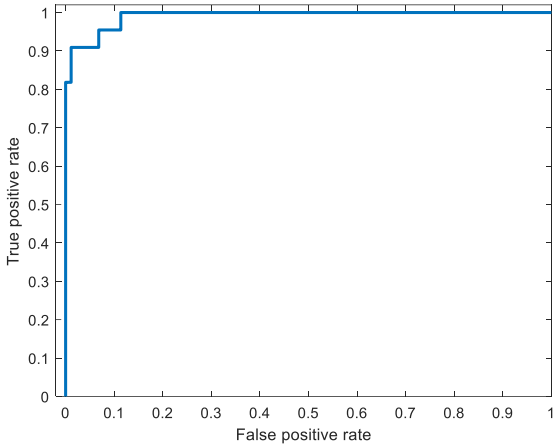

Figure 7. ROC curve for the LDA test

According to Figure 7, the x-axis shows the rate of false positives and the y-axis of the graph shows the rate of true positives, and the curve illustrates how recall (sensitivity) and specificity, which is the percentage of correctness of the negative class in relation to data that are actually negative. By observing the curve shown in Figure 7, it is concluded that the predicted LDA model is able to discriminate well between the two classes, as the curve is close to the upper left corner of the graph, and the area under the ROC curve obtained confirms this good classification, with an value $AUC = 0.9907$.

To improve the classification performance, the multilayer perceptron network was used to classify the database, constituted with an intermediate layer, the weight optimization algorithm used is Adam, the activation function used is rectified linear unit (ReLU), the batch size used to process the samples was 8, the number of epochs was 50, and a learning rate of $\eta = 1 \times 10^{-4}$. Additional information has been added to the database, specifically the Fisher's discriminant function response and the LDA classification.

The test using only the multilayer perceptron network mentioned above consists of an intermediate layer with 2079 neurons, which are the number of parameters of the input data, having as input only the images, where the training database consists of 1002 images and the test database consists of 110 images. The results obtained for the training and testing are presented in Table I.

According to Table I, the perceptron network exhibited better metric values for training than for testing. In addition, it is more efficient at classifying images that report oil slicks on ocean surfaces. The first analysis of the LDA-MLP model uses as input the concatenated vector of images plus the estimate of classes, for the previously specified MLP network that consists of

an intermediate layer with 2080 neurons, which is the number of parameters of the input data with the classification obtained by the LDA. The results of the training and test are listed in Table I.

According to Table I, the LDA-MLP model, using class estimation, was ideal for training because it obtained metrics equal to 100 however, in the test, it presented better values of the metrics, compared with the values obtained for the separate LDA and MLP methods, correcting 100% of the images without oil stains.

The second analysis performed on the LDA-MLP model used the concatenated vector of the image plus the response of the discriminant function as input, for the previously specified MLP network consisting of an intermediate layer of 2080 neurons, which is the number of parameters of the input data with the value obtained by the linear discriminant function. The results obtained for training and testing are listed in Table I.

According to Table I, the LDA-MLP model using the Fisher discriminant function response is satisfactory for detecting and classifying images of oil stains, misclassifying only an image without stain. Of the four tests carried out, it is observed that the LDA-MLP method is more efficient, that is, the information added from the LDA contributed to improve the training of the network, presenting better values for the evaluation metrics, and using the response of the discriminant function is most relevant to training.

Table I. Training and testing metrics for LDA, MLP, LDA-MLP: images plus response and LDA discriminant function

	MODELS							
	LDA		**MLP**		**LDA-MLP LDA Estimation**		**LDA-MLP LDA Discriminant Function**	
METRICS	**Training**	**Test**	**Training**	**Test**	**Training**	**Test**	**Training**	**Test**
Accuracy	100.00	90.00	95.81	93,63	100.00	98.54	100.00	99.09
F1	100.00	93.33	97.38	96.09	100.00	96.47	100.00	99.44
Precision	100.00	100.00	96.29	94.51	100.00	100.00	100.00	98.88
Recall	100.00	87.50	98.48	97.73	100.00	93.18	100.00	100.00

4.5. DL-U-net Model Design

According to the diagram in Figure 3, the procedure for detecting/classifying oil slicks in the DL-U-net model consists of three steps: acquisition of the measurements of the aquatic environment to be monitored, preprocessing of the images, and classification using the U-net network.

The grayscale SAR images have dimensions of 1250×650×3, where 1250 represents the height, 650 represents the width, and 3 represents the depth, which is determined by the number of color channels. The masks also have the same dimensions but in RGB colors. Consequently, the first process is the division of an image into four images to reduce the image dimension to 320×608×3, in addition to increasing the database that started to see four times larger than the real one. In the training database, only the images that reported oil slicks are retained, accounting for 1651 images.

Next, a 5×5 median filter is applied to minimize the speckle noise, that is, to suppress the grainy texture of the images. This filter is applied in both the training and test benches. Figure 8 illustrates the original image and the resulting image from the median filter. After filtering the images, a new bank, called the validation bank was created, containing 100 images taken from the training database.

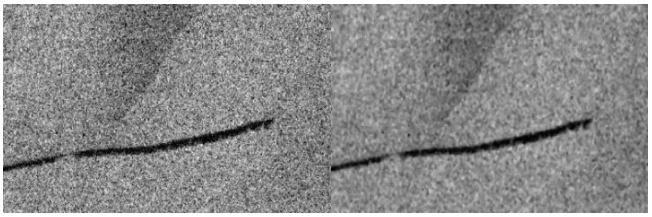

(a) (b)

Figure 8. Resized images: (a) without filter, (b) with median filter

In the masks, the image was divided into four parts, and the RGB images were transformed into grayscale images. Therefore, the oil slicks are represented by pixels with a value of 178. Therefore, with the value of the pixel representing the oil slick, it is possible to exclude all other instances of the image, leaving only the oil slick and ocean surface.

As in the image training database, only the masks corresponding to the images that reported oil slicks remained, accounting for 1651 masks. However, in the test database, this exclusion was not performed; thus, the test mask database consisted of 440 masks.

After performing all the processing, the database is ready to train the U-net network and generate a classifier model that classifies the data with good accuracy. As already mentioned, the U-net network consists of a contraction path and an expansion path, which consists of applying the convolution block four times, consisting of two 3×3 convolutions each, followed by normalization and the rectified linear unit activation function. Another parameter that is determined in the convolution is the padding, which ensures that the layers do not shrink any faster than necessary for the learning of the network. For this network model, it was determined that the output should be the same size as the input. This convolution functioned as a filter that ran through the entire image and captured the most relevant features. These steps are shown in Figure 9, where the input image has dimensions of 320×608×3.

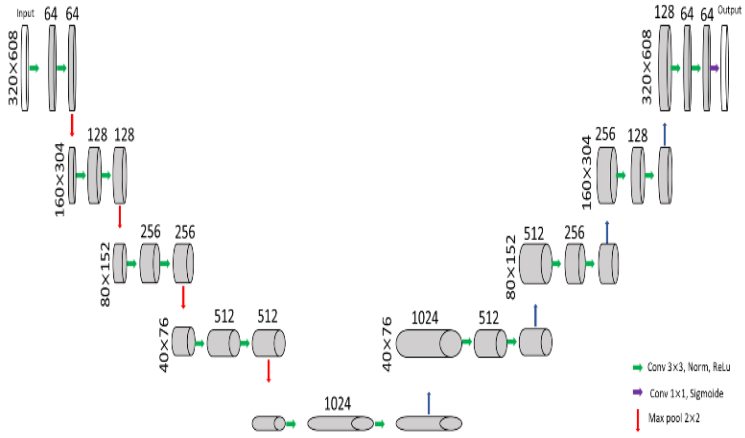

Figure 9. DL-Unet model algorithm

As shown in Figure 9, the DL-U-net model had 64 filters in the first convolution block, 128 in the second, 256 in the third, and 512 in the fourth; that is, it doubled until the last convolution block. After each convolution block, a pooling operation occurs to simplify the information of the previous layer. The method used is the max pooling of area 2×2 with step 2 to reduce the number of weights to be learned and avoid overfitting. After the last max pool, the input image will have dimensions of 20×38×3.

In the expansive path, transposed convolutions need to exist because they use a transformation going in the opposite direction of the normal convolution, that is, from something that has the shape of the output of some convolution to something that has the shape of its input, maintaining a pattern of connectivity compatible with that convolution.

Therefore, this path consisted of four convolution blocks, similar to those used in the contraction path, which changed the number of filters per block to 512, 256, 128, and 64, for blocks 1, 2, 3, and 4, respectively. However, before each convolution block, a transposed convolution was applied with the amount of filter equal to that of the block and dimensions of 2×2 with step 2. The output size has to be the same as the input. In addition to the transposed convolution, it has a concatenation layer.

In the final layer, a 1×1 convolution is used to map each feature vector of 64 components to the desired number of classes, and the activation function used is the sigmoid function, which outputs an image with dimensions of 320×608×3, the same as the input image. Therefore, the network had a total of 23 convolutional layers.

According to the values presented in Table II, the DL-Unet model, with the database without a median filter, indicates that it can learn and precisely classify 84.74% of the test images. This model gives us, in addition to these evaluation metrics, a response image in which the oil slick is detected, as shown in Figure 10.

Figure 10. DL-Unet model response, SAR image, mask and response, respectively

According to Figure 10, first, we have the SAR image, which is the input data for classification. Next, we have the mask, that only reports the presence of oil slick. Finally, we observe the response of the DL-U-net model, which visually appears to closely resemble the mask. For this image, the network achieves an accuracy of 99.88%, an F1 metric of 83.68%, a precision of 75.15%, and a recall of 77.12%. Therefore, it proved to be efficient, even though it had some images representing stains and the surface had no oil stains.

Therefore, to check whether the median filter improves the results, a second analysis was performed, and a database with a 5×5 median filter was used. The training of the DL-U-net network was performed with the Adam optimizer, a learning rate of $\eta = 1 \times 10^{-4}$, a batch size of 8, and 50 epochs. The results obtained in the training had an average precision of 74.08% and an average recall of 64.8%; the test results are presented in Table II.

Table II. Testing metrics for DL-U-net: images without and with median filter

	MODELS	
	DL-U-NET Images without median filter	**DL-U-NET Images with median filter**
METRICS	**Test**	**Test**
Accuracy	98.64	98.94
F1	63.44	61.81
Precision	84.74	72.29
Recall	69.28	81.45

According to the values presented in Table II, the DL-U-net model using a median filter was able to learn and classify the test images with 72.29% precision. This precision is slightly lower than the precision obtained for the database without applying the filter. This network provides as a response the metrics for evaluation and an image that reports the oil slick it detects; that is, an image that attempts to replicate the mask. The closer this response image gets to the mask, the better the network learns, as shown in Figure 11.

Figure 11. DL-U-net model response with median filter, SAR image, mask and response, respectively

Figure 11 appears to have the same image as Figure 10. However, in this case, the training and testing were conducted using the image resulting from a 5×5 median filter. The first image represents the input data that is to be classified, followed by the mask, which indicates only the presence of an oil slick. Finally, we have the response of the DL-U-net model, which visually appears to be less accurate compared to the previous case. However, in terms of the existing oil slick, the model achieved an accuracy of 99.90%, an F1 metric of 88.51%, a precision of 91.49%, and a recall of 85.71%. This shows that it can more accurately detect oil slicks, representing a better response; however, it presents a misdetection as it detects more slicks in the image where they do not exist.

4.6. Performance Analysis of the Classifiers

SAR plays a crucial role in oil slick detection on water surfaces because it can provide high-resolution images, and the detection of these disturbances is possible. The proposed LDA-MLP method integrates the multivariate data analysis technique, LDA, and an artificial neural network (perceptron) to enable oil slick detection on the ocean surface, alerting if an oil spill is detected. The DL-U-net method uses the convolutional neural network with the U-net architecture; however, before training the network, image processing is performed by dividing the image into four images and applying a median filter to eliminate speckle noise, and treating the masks to leave only oil spill instances.

When analyzing the two proposed methods, namely LDA-MLP and DL-U-net, the first method showed better test precision, especially in the test that uses the discriminant function response as one more parameter of the SAR image. Therefore, the LDA-MLP method demonstrated its efficiency and ability to meet expectations, even when compared with other more advanced methods. This highlights those classic techniques, such as LDA and MLP, are still valuable for technological development. In addition, its computational costs are lower compared to more advanced techniques such as DL-U-net, which is more advantageous when embedding this algorithm in a sensor node, for example.

The initial results of the analysis indicated that the two proposed models provided a satisfactory estimate of the detection of oil slicks on the ocean surface, with precisions of 98.88% and 84.74%, respectively. Therefore, the use of discriminant linear analysis to classify the database and use this data as additional information for the database itself, which will train a multilayer perceptron network, proved to be more efficient in detecting oil spills on the surface from the ocean. In addition to the lower computational cost compared to DCNN networks. The two proposed models have been shown to have features to classify images, and both models can be embedded on a microprocessor for local and continuous monitoring of a given environment to prevent disasters to the ecosystem and the population.

4.7. Comparison with others the Classifiers

The work developed in [5] uses the same database, with the same division for training (90%) and testing (10%), and aims to detect oil stains. However, it uses six deep convolutional neural network (DCNN) models to perform semantic segmentation and identify oil spills on the sea surface, and then compares the performance of these models. The selected networks were U-net, LinkNet, PSONet, DeepLabv2, DeepLabv2(msc) and DeepLabv3+, where a learning rate between 5×10^{-5} to 1×10^{-4} was used, the algorithm of the optimization used was also Adam, the batch size used to process the samples was 12, and a random resizing was performed on the training database, increasing the number of images, in addition to rotations. Among the models, the one with the best oil spill detection was the U-net with 53.79%, which is lower than the LDA-MLP method. In addition, the analysis of these new techniques reveals that they are based on classic techniques.

V. CONCLUSION

In this study, methods of analysis and algorithm development for detecting disturbances in aquatic environments were presented. In the first instance, the proposed methodology was evaluated for oil slick detection on the ocean surface using theory, multivariate data analysis, and machine learning approaches. Specifically, MLP-type artificial neural networks and their integration with LDA statistical methods.

The proposed methods were presented from their conception to the characterization and formulation of a specific detection problem to be solved. As part of the methodology, in this study, algorithms and procedures based on machine learning and multivariate data analysis were presented for the development of a unit of the critic module in the detection system.

The deep learning method using the U-net network also proved to be efficient in detecting oil slicks. This presents the advantage of the response image, which is the projection of the slick it detects, making it possible to use this data to carry out other studies, such as the displacement of this slick. However, it has a disadvantage, which is the higher computational cost to train the network.

The proposed LDA-MLP algorithms used simpler methods, and by integrating these two methods, a good result was observed for image classification. In addition, this algorithm did not perform processing in a database. This differs from other studies with SAR images, which, in most cases, first perform processing on the images; for example, a treatment to mitigate the impact of noise. The DL-U-net algorithm, on the other hand, differentiates the image from the detected spot, but it requires more time to train the network, having carried out processing on the image.

ACKNOWLEDGEMENTS

The authors thank to the Federal University of Maranhao (UFMA), National Agency of Petroleum, Natural Gas and Biofuels (ANP), Program of Human Resources Training for the Petroleum, Natural Gas and Biofuels Sector (PRH-ANP), Graduate Program in Electrical Engineering (PPGEE), The Laboratory of Embedded Systems and Intelligent Control (LABSECI), the Coordination for the Improvement of Undergraduate Personnel (CAPES) and the National Council for Scientific and Technological Development (CNPq), for the development infrastructure and financial support.

REFERENCES

[1]. Armin I. Kauerauf, Thomas Hantschel. “Fundamentals of basin and petroleum systems modeling”. 1ª ed. Springer Berlin, Heidelberg, 2009.

[2]. National Agency for Petroleum, Natural Gas and Biofuels, “Oil, Natural Gas and Biofuels Statistical Yearbook 2022.” ANP, 2022. Available in: https://www.gov.br/anp/pt-br/centrais-de-conteudo/publicacoes/anuario-estatistico/oil-natural-gas-and-biofuels-statistical-yearbook-2022.

[3]. V. Paravastu, S. Manoharan and M. Manimaraboopathy, "A proposal of an automatic sensor system for petroleum detection," 2013 International Conference on Green Computing, Communication and Conservation of Energy (ICGCE), Chennai, India, 2013, pp. 335-338, doi: 10.1109/ICGCE.2013.6823456.

[4]. R. R. Selmic, V. V. Phoha, A. Serwadda “Wireless Sensor Networks: Security, Coverage, and Localization,” vol. 69. Ed. Springer, 2016.

[5]. M. Krestenitis, G. Orfanidis, K. Ioannidis, K. Avgerinakis, S. Vrochidis, I. Kompatsiaris. “Oil Spill Identification from Satellite Images Using Deep Neural Networks”. Remote Sens. July 2019, 11(15), 1762; https://doi.org/10.3390/rs11151762.

[6]. Eberhart, R. C., & Shi, Y. (2007). Computational Intelligence: Concepts to Implementations (1st ed.). Morgan Kaufmann.

[7]. D. Song et al., "A Novel Marine Oil Spillage Identification Scheme Based on Convolution Neural Network Feature Extraction From Fully Polarimetric SAR Imagery," in IEEE Access, vol. 8, pp. 59801-59820, 2020, doi: 10.1109/ACCESS.2020.2979219.

[8]. J. F. Hair Jr., W. C. Black, B. J. Babin, R. E. Anderson, R. L. Tatham, "Multivariate Data Analysis", 7ª ed. Pearson New International Edition, 2014.

[9]. Aggarwal, Charu C. "Neural Networks and Deep Learning," 1ª ed. Springer International Publishing, 2018.

[10]. S. Sun et al., "Underwater Image Enhancement With Reinforcement Learning," in IEEE Journal of Oceanic Engineering, doi: 10.1109/JOE.2022.3152519.

[11]. J. S. Suri et al., "UNet Deep Learning Architecture for Segmentation of Vascular and Non-Vascular Images: A Microscopic Look at UNet Components Buffered With Pruning, Explainable Artificial Intelligence, and Bias," in IEEE Access, vol. 11, pp. 595-645, 2023, doi: 10.1109/ACCESS.2022.3232561.

[12]. N. Flood, F. Watson, L. Collett, "Using a U-net convolutional neural network to map woody vegetation extent from high resolution satellite imagery across Queensland, Australia," International Journal of Applied Earth Observation and Geoinformation, vol 82, 2019, https://doi.org/10.1016/j.jag.2019.101897.

[13]. R. O. Duda, P. E. Hart, D. G. Stork, "Pattern Classification," 2nd ed. Wiley-Interscience Publication. Canada: 2001.

[14]. PETROBRAS. "Sustainability Report 2022". Petrobras, 2023. Available in: https://sustentabilidade.petrobras.com.br/en-US/.

[15]. G. Orfanidis, K. Ioannidis, K. Avgerinakis, S. Vrochidis and I. Kompatsiaris, "A Deep Neural Network for Oil Spill Semantic Segmentation in Sar Images," 2018 25th IEEE International Conference on Image Processing (ICIP), Athens, Greece, 2018, pp. 3773-3777, doi: 10.1109/ICIP.2018.8451113.

[16]. L. De Laurentiis, C. E. Jones, B. Holt, G. Schiavon and F. Del Frate, "Deep Learning for Mineral and Biogenic Oil Slick Classification With Airborne Synthetic Aperture Radar Data," in IEEE Transactions on Geoscience and Remote Sensing, vol. 59, no. 10, pp. 8455-8469, Oct. 2021, doi: 10.1109/TGRS.2020.3034722.

[17]. Krestenitis, Marios et al. "Early Identification of Oil Spills in Satellite Images Using Deep CNNs." Conference on Multimedia Modeling (2018).

[18]. D. Song et al., "A Novel Marine Oil Spillage Identification Scheme Based on Convolution Neural Network Feature Extraction From Fully Polarimetric SAR Imagery," in IEEE Access, vol. 8, pp. 59801-59820, 2020, doi: 10.1109/ACCESS.2020.2979219.

[19]. Y. Hu, Z. Jiang, W. Liu, X. Yuan, Q. Hu and J. Wickert, "GNSS-R Sea Ice Detection Based on Linear Discriminant Analysis," in IEEE Transactions on Geoscience and Remote Sensing, vol. 61, pp. 1-12, 2023, Art no. 5800812, doi: 10.1109/TGRS.2023.3269088.

[20]. European Space Agency (ESA). "Sentinel-1". Available in: https://sentinels.copernicus.eu/web/sentinel/home.

[21]. Sousa M. S., Fonseca Neto J. V. da. "Integration of Statistical Methods and Artificial Neural Networks for the Detection of Oil Stains in the Aquatic Environment". ICPRAM, 2023 DOI: 10.5220/0011799300003411.

Authors

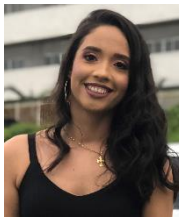

MONIK SILVA SOUSA Master in Electrical Engineering from the Federal University of Maranhão – UFMA (2023), with an emphasis on automation and control, graduated in Electrical Engineering from UFMA (2019). PhD in progress in Electrical Engineering at UFMA (2023-2027), in the area of Automation and Control, with a line of research in Wireless Sensor Network. Currently developing work with Wireless Sensor Network in the Embedded Systems and Intelligent Control Laboratory (LabSECI). With experience in developing teaching aids for Process Control Laboratory and Automation and Control Laboratory.

ALAN DE CARVALHO ARAÚJO Graduated in Electrical Engineering from the Federal University of Maranhão (UFMA), where he did research in the area of control and automation at the UFMA Control and Automation Laboratory. Master in Electrical Engineering from UFMA, in the area of computer science, with a focus on image processing. PhD in progress, in the area of computer science at UFMA. With experience in designing parts in SolidWorks Software, printing parts with a 3D printer, designing electrical installations in AutoCAD Software, machine learning and artificial intelligence.

YAN FERREIRA DA SILVA Graduated in Control and Automation Engineering at Faculdade Pitágoras de São Luis (2017), Master in Electrical Engineering in the area of Automation with an emphasis on Automation and Industrial Process Control at the Federal University of Maranhão - UFMA (2020). PhD in progress, in Electrical Engineering with an emphasis on automation at UFMA (2020-2024). Currently developing work with observers, state estimators based on Deep Reinforcement Learning and Adaptive Dynamic Programming to optimize coverage of dynamic nodes, detection and tracking of targets in WSNs (Wireless Sensor Network) at LabSECI (Embedded Systems and Intelligent Control Laboratory) - UFMA.

ARISTÓFANES CORRÊA SILVA Graduated in Computer Science from the Federal University of Maranhão (1995), Master's degree in Electrical Engineering from the Federal University of Maranhão (1997) and PhD in Informatics from the Pontifical Catholic University of Rio de Janeiro (2004). He is currently a full professor at the Federal University of Maranhão (UFMA). He has experience in the area of Computer Science, with an emphasis on Graphics Processing, working mainly on the following topics: medical images and artificial intelligence.

ALCIONE MIRANDA DOS SANTOS Graduated in Statistics from the Federal University of Pernambuco (1991), master's degree in Statistics from the Federal University of Rio de Janeiro (1996) and PhD in Production Engineering from the Federal University of Rio de Janeiro (2003). She is currently a professor at the Department of Public Health at the Federal University of Maranhão (DSP-UFMA), where she has been developing research activities in the following areas of Data Science and Statistics: Survival Analysis, Item Response Theory and Machine Learning. Permanent professor of the Postgraduate Program in Public Health-UFMA and Coordinator of the Biomedical Informatics Center at DSP-UFMA.

JOÃO VIANA DA FONSECA NETO Full professor at the Federal University of Maranhão. He holds a degree in Electrical Engineering from the Federal University of Paraíba (1982), a master's degree in Electrical Engineering from the Federal University of Paraíba (1986), and a PhD in Electrical Engineering from the State University of Campinas (2000). Currently, he develops research in Computational Intelligence with a focus on fusing the approaches of artificial neural networks, evolutionary computing, fuzzy logic for identification and control of real-world dynamic systems. His research is focused on online tuning and selection of optimal controllers for MIMO systems.